Current Biology 24, 1542–1547, July 7, 2014 ©2014 Elsevier Ltd All rights reserved http://dx.doi.org/10.1016/j.cub.2014.05.049

Report

Dynamics of Neural Population Responses in Prefrontal Cortex Indicate Changes of Mind on Single Trials

Roozbeh Kiani,[1,2,4,*] Christopher J. Cueva,[2,4] John B. Reppas,[2] and William T. Newsome[2,3]
[1]Center for Neural Science, New York University, 4 Washington Place, Room 809, New York, NY 10003, USA
[2]Department of Neurobiology, Stanford University School of Medicine, Fairchild Building D209, Stanford, CA 94305, USA
[3]Howard Hughes Medical Institute, Stanford University School of Medicine, Beckman Center, 279 Campus Drive, Room B202, Stanford, CA 94305, USA

Summary

Decision making is a complex process in which different sources of information are combined into a decision variable (DV) that guides action [1, 2]. Neurophysiological studies have typically sought insight into the dynamics of the decision-making process and its neural mechanisms through statistical analysis of large numbers of trials from sequentially recorded single neurons or small groups of neurons [3–6]. However, detecting and analyzing the DV on individual trials has been challenging [7]. Here we show that by recording simultaneously from hundreds of units in prearcuate gyrus of macaque monkeys performing a direction discrimination task, we can predict the monkey's choices with high accuracy and decode DV dynamically as the decision unfolds on individual trials. This advance enabled us to study changes of mind (CoMs) that occasionally happen before the final commitment to a decision [8–10]. On individual trials, the decoded DV varied significantly over time and occasionally changed its sign, identifying a potential CoM. Interrogating the system by random stopping of the decision-making process during the delay period after stimulus presentation confirmed the validity of identified CoMs. Importantly, the properties of the candidate CoMs also conformed to expectations based on prior theoretical and behavioral studies [8]: they were more likely to go from an incorrect to a correct choice, they were more likely for weak and intermediate stimuli than for strong stimuli, and they were more likely earlier in the trial. We suggest that simultaneous recording of large neural populations provides a good estimate of DV and explains idiosyncratic aspects of the decision-making process that were inaccessible before.

Results

Psychophysical studies of the decision-making process in various contexts suggest an underlying neural mechanism based on integration of evidence toward a decision criterion [11–17]. Supporting evidence for this mechanism has emerged from electrophysiological studies of the parietal cortex, frontal cortex, basal ganglia, and superior colliculus of monkeys performing simple perceptual decisions [3, 5, 18–22]. More recently, magnetoencephalography, electroencephalography, and functional magnetic resonance imaging studies have revealed homologous mechanisms in the human brain [23–26].

Although these studies have significantly advanced our understanding of the decision-making process, they have mainly relied on statistical analyses across trials because of the stochastic nature of spiking activity at the single-neuron level. Yet tracking the evolution of the decision variable (DV) on single trials and relating fluctuations in the DV to internal cognitive states and overt behavior are critical for incisive tests of current models of decision making. Recent advances in multielectrode recording promise to break this barrier through measurement and analysis of the underlying neural population responses on single trials. So far, this ability has been mainly used in the field of neural prosthetics, where accurate, real-time decoding of neural population responses is necessary for guidance of motor prosthetic devices (e.g., [27, 28]). However, similar techniques can also be used to advance our understanding of cognitive processes, especially decision making [7, 29].

We used 96-channel multielectrode arrays to record from neural populations in area 8Ar of the prearcuate gyrus of two macaque monkeys while they performed a direction discrimination task [30, 31] (Figure 1A). On each trial, the monkey viewed a patch of randomly moving dots for 800 ms. After a delay period of variable length, the monkey received the "go" cue and reported the perceived motion direction by making a saccadic eye movement to one of the two available targets (T1 and T2). The multielectrode array covered 4 mm × 4 mm of the cortical surface (Figure 1B) and enabled us to record simultaneously from hundreds of single- and multineuron units in a significant portion of the prearcuate gyrus. Compatible with previous studies, many units showed differential activity for the two choices during the motion viewing and delay periods [20, 32], in addition to the perisaccadic period [33] (Figure 1C).

To explore the efficacy of simultaneous, high-density recording for analyzing dynamics of the decision-making process, we trained a logistic classifier to predict the monkey's upcoming choice based on neural population responses at successive times during individual trials (100 ms sliding window; see the Supplemental Experimental Procedures). The classifier finds a set of linear weights ($\vec{w}$) on the population neural responses ($\vec{r}$) that maximizes the probability of correctly predicting the choice. Although it is possible to improve the prediction accuracy by adopting more-sophisticated nonlinear models, in this report we adhere to the linear model for its simplicity and biological plausibility. Other models yielded qualitatively similar results. Figure 2A shows the cross-validated accuracy (see the Supplemental Experimental Procedures) of our model, averaged across sessions. Model prediction accuracy is near chance at the beginning of the trial but rises quickly ~200 ms after motion onset, reaching perfection just before the saccade.

Across 15 data sets, the prediction accuracy of the population responses was much higher than that of the average single unit (Figure 2B). In the 100 ms window immediately before the "go" cue, the cross-validated accuracy of

[4]Co-first author
*Correspondence: roozbeh@nyu.edu

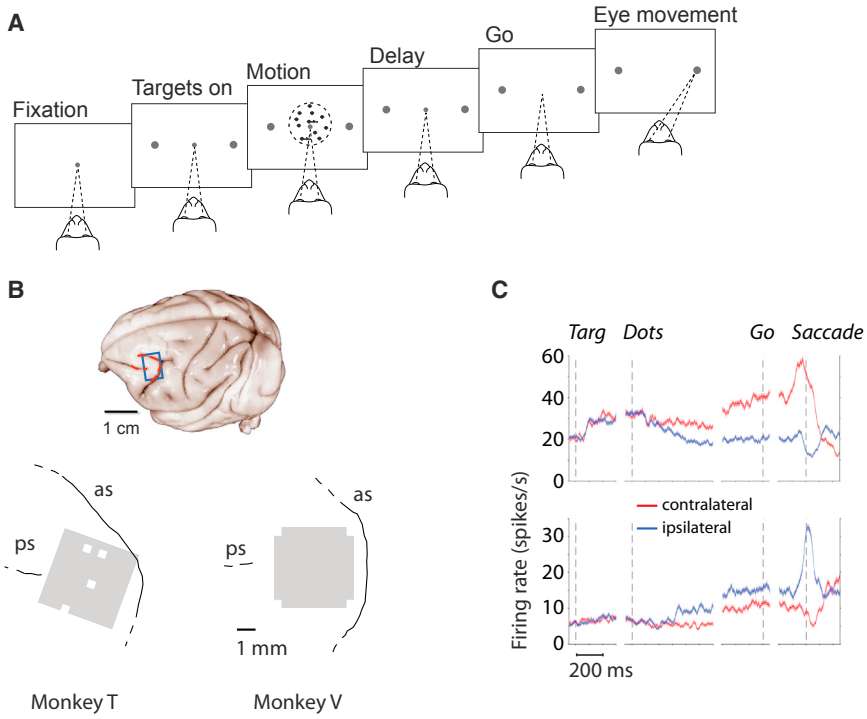

Figure 1. Multielectrode Recording from the Prearcuate Gyrus during a Direction Discrimination Task

(A) Behavioral task. The monkey views 800 ms of random dot motion while maintaining its gaze on a central fixation point. The strength and direction of motion varied randomly from trial to trial. After a variable delay period, the monkey received the "go" signal (fixation point disappeared) and reported the perceived motion direction with a saccadic eye movement to one of two visual targets. Correct responses were rewarded with juice after a short hold period.

(B) Two macaque monkeys were implanted with multichannel electrode arrays in the prearcuate gyrus, which is marked with a blue box on the lateral surface of a typical macaque brain (top; University of Wisconsin Brain Collection). The exact location of each array with respect to the arcuate (as) and principal (ps) sulci is shown for each monkey (bottom). The white squares on the array show the locations of the ground pins. The portions of the principal and arcuate sulci that were visible in the craniotomy are indicated with black lines. Dashed segments at the end of a sulcus indicate that the sulcus extended in that direction beyond our window of visibility.

(C) Average responses of two example prearcuate units for correct ipsilateral and contralateral choices. The units were recorded from the same electrode in the same session but had different motion and saccade selectivities. Shading indicates mean ± SEM.

the population prediction was close to 0.9 on average (mean ± SEM: 0.86 ± 0.01), whereas the average accuracy of individual units was barely above chance (mean ± SEM: 0.557 ± 0.001) and was significantly smaller than that of the population (t test, $p < 10^{-8}$). More importantly, not only was population performance better than the average single unit, but it was consistently superior to the best unit recorded in each session (Figure 2C; t test, $p = 3 \times 10^{-5}$). The population was superior to individual units in other time epochs as well (data not shown).

The increased prediction accuracy afforded by multielectrode recording enabled more accurate tracking of the decision variable over time. In essence, our logistic regression finds the best hyperplane that separates the population response patterns associated with the two choices. The population response pattern at each moment can be envisioned as a point in a high-dimensional space whose axes are the firing rates of individual units. The distance of this point from the discriminant hyperplane $(\vec{w}^T \vec{r})$ represents the strength of model's prediction: a small distance corresponds to low certainty about the monkey's upcoming choice, and a large distance corresponds to high certainty. We call this distance "model decision variable." The model DV provides an estimate of the monkey's internal DV, especially when the model prediction accuracy is high. Averaged across trials, the model DV gradually increased from zero to large values (positive and negative values corresponded to T1 and T2 predictions, respectively; Figure 3A). The rate of this rise depended on the strength of motion, especially during the motion-viewing period (Figure 3A, inset): DV increased more rapidly for stronger stimuli, compatible with previous observations in parietal and prefrontal neurons, where the rate of change of neural responses depends on the strength of sensory evidence [3, 6, 20, 34, 35].

Similarly, on individual trials, the DV fluctuated around the discriminant hyperplane at the beginning of the motion-viewing period but gradually moved farther from the hyperplane over time. After gaining an initial distance, the population-based DV typically stayed on one side of the hyperplane during the late motion-viewing period and the ensuing delay (Figure 3B, two example trials). On a minority of trials, however, the population response crossed from one side of the hyperplane to the other side during the trial, signaling a shift in the predicted choice from one target to the other (Figure 3C, two example trials).

An intriguing possibility is that these changes in DV sign, calculated from the neural population response, identify changes of mind (CoMs) that occur in human and animal observers as they make choices on the basis of variable evidence [7–10]. Alternatively, however, changes in sign of the DV might simply reflect noise from any number of sources that are irrelevant to performance on the task.

We conducted four analyses to test whether observed variations in the DV reflect, at least in part, genuine changes of mind. The first analysis concerns the reliability of DV fluctuations for monitoring the momentary "decision state" of the system as time passes during long-duration trials. The remaining three analyses assess whether intratrial DV sign changes conform to change-of-mind properties that are predicted by decision-making models and empirically observed in humans and monkeys performing a similar decision-making task.

Prediction of Choice Is Reliable throughout Long Delay Periods

The initial important question is whether intratrial sign changes in the DV, like those illustrated in Figure 3C, are simply noise or whether they accurately reflect moment-to-moment variation in the decision state of the system—the decision that would

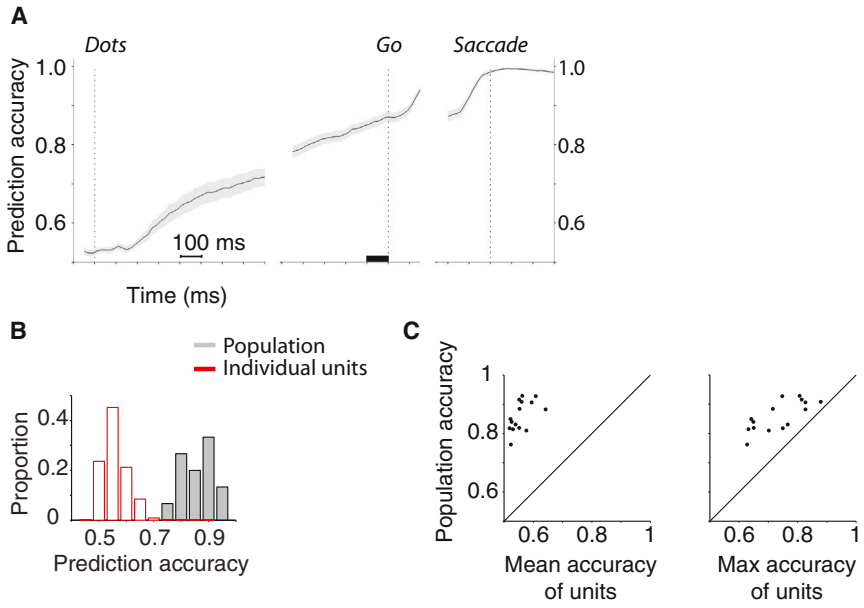

Figure 2. The Recorded Neural Populations Afford High Accuracy Prediction of the Monkeys' Choices

(A) Prediction accuracy of the recorded population for the monkey's choice. A logistic model was fit to 90% of the trials in each session and was used to predict the choice in the remaining 10%, in sliding 100 ms bins. The dark trace and shading indicate mean ± SEM across the sessions. The horizontal black bar indicates the time window that was used in the analyses in (B) and (C).

(B) The neural population classifier is a better predictor of the monkey's choice than the average of the individual units recorded in a session. The probability densities of population and individual unit choice prediction accuracies are highly distinct. Prediction accuracies were calculated for a 100 ms window immediately before the "go" cue.

(C) Comparison of population choice prediction accuracy with the mean (left) and best (right) individual units. Each point represents one data collection session. Even the best individual units are inferior to the population.

be made if the trial were to end *now*. We addressed this question by separately analyzing predictive accuracy of the population activity for trials of different delay period duration. During each experiment, the duration of the delay period was varied randomly among several preset values (see the Supplemental Experimental Procedures). We grouped the trials into quintiles based on the length of the delay period. For each quintile, we then calculated the hyperplane that best separated the T1 and T2 choice trials from the pattern of neural population response in the 100 ms immediately *before* the "go" cue. For all quintiles, the model achieved high cross-validated accuracies for predicting the monkey's choice on individual trials (Figure 4A; 0.76 ± 0.02 for the shortest delays to 0.87 ± 0.02 for the longest delay). The results were not critically dependent on using a separate model for each quintile; similar results were obtained when a single model was used for all quintiles (Figure S1 available online). Although predictive accuracy improved modestly for longer delay periods, it was far above chance even for the shortest delays. Thus, the sign of the DV during the delay period is a good predictor of choice, even for the shortest-duration trials.

Importantly, there is no distinction between long- and short-duration trials prior to the first possible "go" signal—the temporal structures of the trials are identical until that point. Thus, predictive accuracy of the DV sign measured prior to the "go" signal on shorter-duration trials provides an objective estimate of predictive accuracy on longer-duration trials *had those trials ended at an earlier point in time*. We therefore conclude that DV sign changes on longer-duration trials (e.g., Figure 3C) provide insight into the momentary decision state of the system, reflecting in part choices that would have been made had we terminated the trial earlier.

DV Sign Changes Reflect Expected Properties of Behavioral Changes of Mind

After identifying candidate CoMs using DV sign changes, we performed three analyses to determine whether candidate CoMs exhibit properties that are associated with actual CoMs in behavioral studies and are expected from current models of the decision process [7, 8].

First, CoMs should happen more frequently for weak- and intermediate-strength motion stimuli than for strong motion stimuli because counterevidence that elicits a CoM will occur less frequently for stronger stimuli [8]. Figure 4B shows that the predicted trend is indeed present in our data (Equation S3 in the Supplemental Experimental Procedures, $\beta_1 = -0.23 \pm 0.04$, $p = 1.6 \times 10^{-8}$).

Second, CoMs are more likely to steer the decision from an incorrect to a correct option than vice versa because they are based on evidence that is not yet processed during the initial stages of choice formation [8, 9]. On average, incorporation of additional evidence should improve the decision maker's accuracy. Consistent with this prediction, we observed that candidate CoMs derived from our neural population data were more likely to shift the predicted choices from the incorrect target to the correct target (Figure 4C). The difference in CoM toward correct versus wrong choices was significantly larger than zero (sign test, $p < 10^{-8}$) and grew as a function of motion strength (Equation S4 in the Supplemental Experimental Procedures, $\beta_1 = 0.19 \pm 0.07$, $p = 0.009$). Thus, CoMs increased the monkey's overall reward intake. We also tested whether the monkey's final choices after CoMs were more likely to be correct compared to the trials in which CoMs were not detected. Controlling for motion strength and delay duration, we found no significant difference between the two trial types (Equation S5 in the Supplemental Experimental Procedures, $\beta_2 = -0.004 \pm 0.043$, $p = 0.92$). Since CoMs improved the probability of a correct response, they must have occurred selectively on trials for which the initial decision state was likely to be incorrect, perhaps due to lapses of attention earlier in the trial.

Third, the probability of a CoM should decrease as the monkey waits during the delay period. Due to the finite latency of visual signals, processing the last sensory evidence necessarily occurs during the delay period, and memory processes related to the visual stimulus may influence the final decision as well. As the delay period proceeds, however, a final commitment to a choice is increasingly likely. Consistent with this hypothesis, we observed a monotonic decline in the probability of a CoM with delay period duration (Figure 4D;

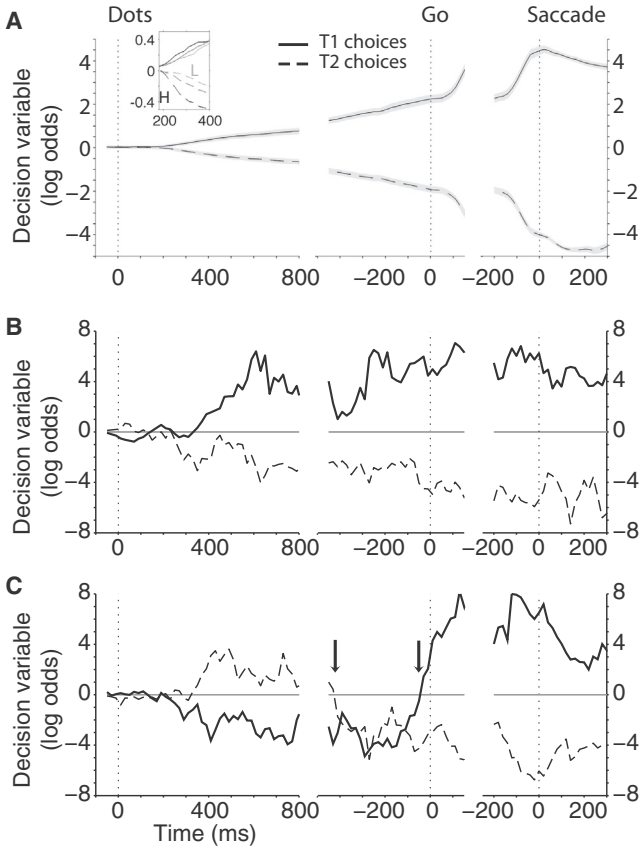

Figure 3. The Model Decision Variable Indicates Accumulation of Evidence over Time, and Intratrial Changes in the Sign of the DV Identify Candidate Changes of Mind

A logistic regression (Equation S1 in the Supplemental Experimental Procedures) was used to find the best hyperplane that separates the population response patterns corresponding to the two choices. The distance of the population response pattern from this discriminant hyperplane represents the model belief about the upcoming choice. We call this distance the model decision variable, or DV.

(A) Average decision variable across the sessions. The inset shows that the buildup of the decision variable during the motion-viewing period depends on stimulus strength (H, motion strength $\geq$ 20%; L, motion strength $\leq$ 6%). The dark traces and shading represent the mean ± SEM.

(B) Two sample trials in which the model DV built up to a positive (solid) or negative (dashed) value and maintained its sign throughout the trial. The trials ended with T1 and T2 choices, respectively.

(C) Two sample trials in which the sign of the model DV flipped during the delay period, indicating a change of predicted choice based on the model. Arrows indicate the time of flip.

Equation S6 in the Supplemental Experimental Procedures, $\beta_2 = -0.21 \pm 0.01$, $p < 10^{-8}$).

The success of the model for the delay period encouraged us to investigate the properties of candidate CoMs during the motion-viewing interval as well, even though success was less certain for two reasons. First, because we used a constant stimulus duration in all experiments, we were unable to validate candidate CoMs during motion viewing using short-duration trials as described above for the delay period. Second, candidate CoMs were less reliable during motion viewing as reflected in the lower predictive power of the model during this interval (Figure 2A). Nevertheless, the properties of candidate CoMs during the motion-viewing interval were similar to those during the delay period. CoMs were less frequent for stronger stimuli (Figure S2A; Equation S3 in the Supplemental Experimental Procedures, $\beta_1 = -0.064 \pm 0.021$, $p = 0.003$) and were more likely to change the DV in the direction of a correct judgment (Figure S2B; Equation S4 in the Supplemental Experimental Procedures, $\beta_1 = 0.71 \pm 0.18$, $p = 0.001$). The frequency of candidate CoMs at the beginning of the motion-viewing period was low because the DV is initially near chance and must first build up toward one of the choices before a CoM can be detected reliably (see the Supplemental Experimental Procedures). Thus, CoM frequency increased initially but declined after 300 ms of motion viewing (Figure S2C) due to increased likelihood of commitment to a choice, consistent with the delay period results (Figure 4D). These results from the motion-viewing period are encouraging but should be interpreted cautiously because of sensitivity of some results (Figure S2C) to time window sizes (see the Supplemental Experimental Procedures).

Overall, candidate CoMs identified from high-density recordings of prefrontal cortex conform to all three predictions based on behavioral analysis of changes of mind.

Discussion

Neurophysiological studies have typically sought insight into the dynamics of decision making and its neural mechanisms through statistical analysis of large numbers of trials from sequentially recorded single neurons or small groups of neurons. Measurement and analysis of the DV on individual trials has been challenging due to technical and conceptual limitations. We sought to overcome these limitations by (1) recording simultaneously from hundreds of units in cortical areas hypothesized to contribute to the decision-making process, (2) developing simple, efficient algorithms for estimation of the covert DV from neural population responses, and (3) implementing a new analytic approach to verify the accuracy of the estimated DV fluctuations during the delay period.

The ability to track moment-to-moment variation of the DV enables the study of important aspects of the decision-making process that have been largely inaccessible thus far. As a proof of concept, we focused on changes of mind during perithreshold judgments of motion direction. Our behavioral task created fertile conditions for CoMs due to the noisy, temporally extended nature of the visual motion stimulus. Our first new finding is that the covert DV can be accurately tracked during single behavioral trials using the methods introduced in this paper. Crucially, trials with short delay periods verify the accuracy of estimates of the covert DV on longer trials; in essence, short-delay trials act as "probes" of ongoing DV estimates on longer trials [34, 36, 37]. Our second new finding is that changes in the sign of the DV identify candidate CoMs and that candidate CoMs conform to three different predictions based on prior behavioral and modeling studies. Together, these results demonstrate the power of high-density neural recordings for single-trial estimates of the fluctuating DV and for detection of covert changes in decision state commonly referred to as changes of mind.

CoMs can arise from various sources: changing sensory evidence [8], correction of an initial confusion about stimulus-response association [9], incorporation of a new decision policy, or retrieval of new information from memory [8]. Our monkeys' CoMs may stem from any of these sources or others, such as simple lapses in attention or effort. Accumulated over time, CoMs tend to be self-corrections, often benefitting the decision maker by improving accuracy. By characterizing

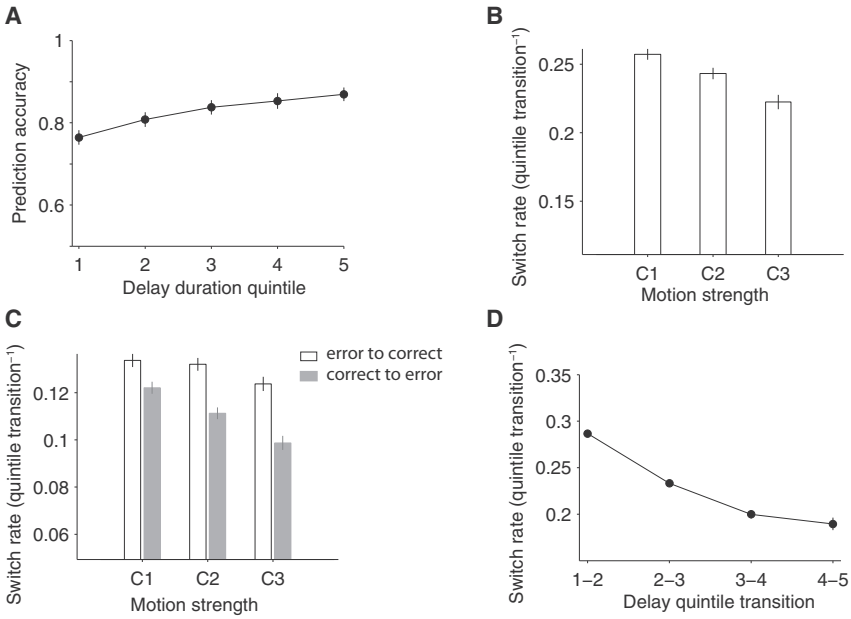

Figure 4. The Sign of the Model DV Reliably Reflects the Incipient Decision throughout the Delay Period

Intratrial changes in the sign of the DV conform to CoM properties expected from theoretical and behavioral studies.

(A) Cross-validated prediction accuracy of the monkey's choice for different delay durations. Trials were grouped into quintiles based on delay period duration. Accurate choice prediction on short-duration trials confirms that variation in DV reflects the monkey's decision state at early points in long-duration trials. Thus, intratrial changes in DV sign are consistent with CoM as opposed to extraneous noise (see the Results).

(B) Probability of switching from one predicted choice to another in consecutive delay quintiles declines for stronger motion (C_1, motion strength $\leq$ 6%; C_2, 6% < motion strength $\leq$ 20%; C_3, motion strength > 20%).

(C) Switches in the predicted choice were more likely to rectify an erroneous choice, especially for stronger motion stimuli.

(D) Switches were more frequent early during delay.

Error bars indicate the SEM. See also Figures S1 and S2.

the neural DV and identifying CoMs on individual trials, we show that monkeys, like humans, exhibit self-correcting behavior.

Past studies have documented cortical and subcortical fluctuations in neural activity that might correspond to changes of mind [7, 29, 38]. Those studies focused on the detection of discrete hidden states in the responses of single neurons [38] or small numbers of simultaneously recorded neurons [7, 29]. The discrete states are defined as specific patterns of spiking across the recorded population. Transitions from one state to another —often formalized by a hidden Markov model—can occasionally signal changes of mind. Here we extend those studies by extracting a continuous measure of the DV, characterizing its dynamics, and confirming the inferred CoMs by interrogating the monkey's choice at variable times.

The probabilistic characterization of the choice provides an analog estimation of the DV, compatible with the quantitative models of the decision-making process [12, 17, 35, 39]. In those models, sources of information are integrated into an analog variable [31] that explains both the choice and reaction time. However, it remains to be seen whether various factors, such as priors and value information, that bear on the decision in those models also modify our estimated DV.

Our model incorporates the responses of all neurons recorded on the array in a given experiment. Unlike in many classic single-neuron studies, we did not focus on merely the units that were highly selective for the motion directions or target locations used in the task [20, 40, 41]. We do not know whether all of the recorded neurons contributed to the decision-making process. Nor do we know the exact role that they may play in the process. However, the recorded neurons are informative about the monkey's upcoming action as indicated by the model's high prediction accuracy. We simply exploit this information to provide a probabilistic glimpse into the DV that supports choice and CoM. Our model is not a mechanistic account of how the DV is constructed or how commitment to a choice is made. Addressing those questions requires further experiments and selective recording and manipulation of neurons based on their response selectivity (e.g., [18, 34, 42–44]).

The advent of techniques for routine, simultaneous recording of tens to hundreds of neurons offers unique opportunities for cognitive neuroscience, particularly for the detection and tracking of cognitive states and processes that occur unpredictably in time and have no overt behavioral correlate. Covert cognitive processes are difficult to monitor in classical neurophysiological studies that require time-locking and across-trial signal averaging, but they are potentially detectable in real time from neural population activity. Even when covert neural processes are detectable, however, their interpretation will depend on creative strategies for behavioral verification. Our study of CoM offers a first step in that direction.

Supplemental Information

Supplemental Information includes Supplemental Experimental Procedures and two figures and can be found with this article online at http://dx.doi.org/10.1016/j.cub.2014.05.049.

Author Contributions

R.K. and W.T.N. developed the concept. J.B.R. collected the data. R.K. designed the analyses. R.K. and C.J.C. implemented the analyses. R.K. and W.T.N. wrote the paper.

Acknowledgments

We thank K. Shenoy, M. Kaufman, D. Kimmel, V. Mante, D. Peixoto, V. McGinty, and M. Churchland for helpful discussions, and we thank Jamie Sanders, Jessica Powell, Sania Fong, and Julian Brown for technical assistance throughout the project. We are particularly grateful to Stephen Ryu, who was the primary surgeon for the array implants. This research was supported by the Howard Hughes Medical Institute, the Air Force Research Laboratory (agreement number FA9550-07-1-0537), a Berry Postdoctoral Fellowship to R.K., and a Sloan Research Fellowship to R.K.

Received: April 21, 2014
Revised: May 20, 2014
Accepted: May 21, 2014
Published: June 19, 2014

References

1. Platt, M.L., and Glimcher, P.W. (1999). Neural correlates of decision variables in parietal cortex. Nature *400*, 233–238.
2. Shadlen, M.N., and Newsome, W.T. (1996). Motion perception: seeing and deciding. Proc. Natl. Acad. Sci. USA *93*, 628–633.
3. Shadlen, M.N., and Newsome, W.T. (2001). Neural basis of a perceptual decision in the parietal cortex (area LIP) of the rhesus monkey. J. Neurophysiol. *86*, 1916–1936.
4. Hussar, C.R., and Pasternak, T. (2013). Common rules guide comparisons of speed and direction of motion in the dorsolateral prefrontal cortex. J. Neurosci. *33*, 972–986.
5. Heitz, R.P., and Schall, J.D. (2012). Neural mechanisms of speed-accuracy tradeoff. Neuron *76*, 616–628.
6. de Lafuente, V., and Romo, R. (2006). Neural correlate of subjective sensory experience gradually builds up across cortical areas. Proc. Natl. Acad. Sci. USA *103*, 14266–14271.
7. Bollimunta, A., Totten, D., and Ditterich, J. (2012). Neural dynamics of choice: single-trial analysis of decision-related activity in parietal cortex. J. Neurosci. *32*, 12684–12701.
8. Resulaj, A., Kiani, R., Wolpert, D.M., and Shadlen, M.N. (2009). Changes of mind in decision-making. Nature *461*, 263–266.
9. Rabbitt, P.M. (1966). Errors and error correction in choice-response tasks. J. Exp. Psychol. *71*, 264–272.
10. Albantakis, L., Branzi, F.M., Costa, A., and Deco, G. (2012). A multiple-choice task with changes of mind. PLoS ONE *7*, e43131.
11. Link, S.W. (1992). The Wave Theory of Difference and Similarity (Hillsdale: Erlbaum).
12. Smith, P.L., and Ratcliff, R. (2004). Psychology and neurobiology of simple decisions. Trends Neurosci. *27*, 161–168.
13. Laming, D.R.J. (1968). Information Theory of Choice Reaction Time (New York: Wiley).
14. Luce, R.D. (1986). Response Times: Their Role in Inferring Elementary Mental Organization (Belfast: Oxford University Press).
15. Carpenter, R.H., Reddi, B.A., and Anderson, A.J. (2009). A simple two-stage model predicts response time distributions. J. Physiol. *587*, 4051–4062.
16. Krajbich, I., and Rangel, A. (2011). Multialternative drift-diffusion model predicts the relationship between visual fixations and choice in value-based decisions. Proc. Natl. Acad. Sci. USA *108*, 13852–13857.
17. Shadlen, M.N., and Kiani, R. (2013). Decision making as a window on cognition. Neuron *80*, 791–806.
18. Bollimunta, A., and Ditterich, J. (2012). Local computation of decision-relevant net sensory evidence in parietal cortex. Cereb. Cortex *22*, 903–917.
19. Horwitz, G.D., and Newsome, W.T. (1999). Separate signals for target selection and movement specification in the superior colliculus. Science *284*, 1158–1161.
20. Kim, J.N., and Shadlen, M.N. (1999). Neural correlates of a decision in the dorsolateral prefrontal cortex of the macaque. Nat. Neurosci. *2*, 176–185.
21. Ratcliff, R., Hasegawa, Y.T., Hasegawa, R.P., Smith, P.L., and Segraves, M.A. (2007). Dual diffusion model for single-cell recording data from the superior colliculus in a brightness-discrimination task. J. Neurophysiol. *97*, 1756–1774.
22. Ding, L., and Gold, J.I. (2013). The basal ganglia's contributions to perceptual decision making. Neuron *79*, 640–649.
23. Donner, T.H., Siegel, M., Fries, P., and Engel, A.K. (2009). Buildup of choice-predictive activity in human motor cortex during perceptual decision making. Curr. Biol. *19*, 1581–1585.
24. O'Connell, R.G., Dockree, P.M., and Kelly, S.P. (2012). A supramodal accumulation-to-bound signal that determines perceptual decisions in humans. Nat. Neurosci. *15*, 1729–1735.
25. Kayser, A.S., Buchsbaum, B.R., Erickson, D.T., and D'Esposito, M. (2010). The functional anatomy of a perceptual decision in the human brain. J. Neurophysiol. *103*, 1179–1194.
26. Heekeren, H.R., Marrett, S., Bandettini, P.A., and Ungerleider, L.G. (2004). A general mechanism for perceptual decision-making in the human brain. Nature *431*, 859–862.
27. Gilja, V., Nuyujukian, P., Chestek, C.A., Cunningham, J.P., Yu, B.M., Fan, J.M., Churchland, M.M., Kaufman, M.T., Kao, J.C., Ryu, S.I., and Shenoy, K.V. (2012). A high-performance neural prosthesis enabled by control algorithm design. Nat. Neurosci. *15*, 1752–1757.
28. Arce, F.I., Lee, J.C., Ross, C.F., Sessle, B.J., and Hatsopoulos, N.G. (2013). Directional information from neuronal ensembles in the primate orofacial sensorimotor cortex. J. Neurophysiol. *110*, 1357–1369.
29. Lemus, L., Hernández, A., Luna, R., Zainos, A., Nácher, V., and Romo, R. (2007). Neural correlates of a postponed decision report. Proc. Natl. Acad. Sci. USA *104*, 17174–17179.
30. Britten, K.H., Shadlen, M.N., Newsome, W.T., and Movshon, J.A. (1992). The analysis of visual motion: a comparison of neuronal and psychophysical performance. J. Neurosci. *12*, 4745–4765.
31. Kiani, R., Churchland, A.K., and Shadlen, M.N. (2013). Integration of direction cues is invariant to the temporal gap between them. J. Neurosci. *33*, 16483–16489.
32. Mante, V., Sussillo, D., Shenoy, K.V., and Newsome, W.T. (2013). Context-dependent computation by recurrent dynamics in prefrontal cortex. Nature *503*, 78–84.
33. Chafee, M.V., and Goldman-Rakic, P.S. (1998). Matching patterns of activity in primate prefrontal area 8a and parietal area 7ip neurons during a spatial working memory task. J. Neurophysiol. *79*, 2919–2940.
34. Kiani, R., Hanks, T.D., and Shadlen, M.N. (2008). Bounded integration in parietal cortex underlies decisions even when viewing duration is dictated by the environment. J. Neurosci. *28*, 3017–3029.
35. Purcell, B.A., Heitz, R.P., Cohen, J.Y., Schall, J.D., Logan, G.D., and Palmeri, T.J. (2010). Neurally constrained modeling of perceptual decision making. Psychol. Rev. *117*, 1113–1143.
36. Thura, D., and Cisek, P. (2014). Deliberation and commitment in the premotor and primary motor cortex during dynamic decision making. Neuron *81*, 1401–1416.
37. Stanford, T.R., Shankar, S., Massoglia, D.P., Costello, M.G., and Salinas, E. (2010). Perceptual decision making in less than 30 milliseconds. Nat. Neurosci. *13*, 379–385.
38. Horwitz, G.D., and Newsome, W.T. (2001). Target selection for saccadic eye movements: prelude activity in the superior colliculus during a direction-discrimination task. J. Neurophysiol. *86*, 2543–2558.
39. Green, D.M., and Swets, J.A. (1966). Signal Detection Theory and Psychophysics (New York: Wiley).
40. Schall, J.D., and Hanes, D.P. (1993). Neural basis of saccade target selection in frontal eye field during visual search. Nature *366*, 467–469.
41. Zaksas, D., and Pasternak, T. (2006). Directional signals in the prefrontal cortex and in area MT during a working memory for visual motion task. J. Neurosci. *26*, 11726–11742.
42. Hanks, T.D., Ditterich, J., and Shadlen, M.N. (2006). Microstimulation of macaque area LIP affects decision-making in a motion discrimination task. Nat. Neurosci. *9*, 682–689.
43. Salzman, C.D., Murasugi, C.M., Britten, K.H., and Newsome, W.T. (1992). Microstimulation in visual area MT: effects on direction discrimination performance. J. Neurosci. *12*, 2331–2355.
44. Law, C.T., and Gold, J.I. (2008). Neural correlates of perceptual learning in a sensory-motor, but not a sensory, cortical area. Nat. Neurosci. *11*, 505–513.

Current Biology, Volume *24*

Supplemental Information

Dynamics of Neural Population Responses in Prefrontal Cortex Indicate Changes of Mind on Single Trials

Roozbeh Kiani, Christopher J. Cueva, John B. Reppas, and William T. Newsome

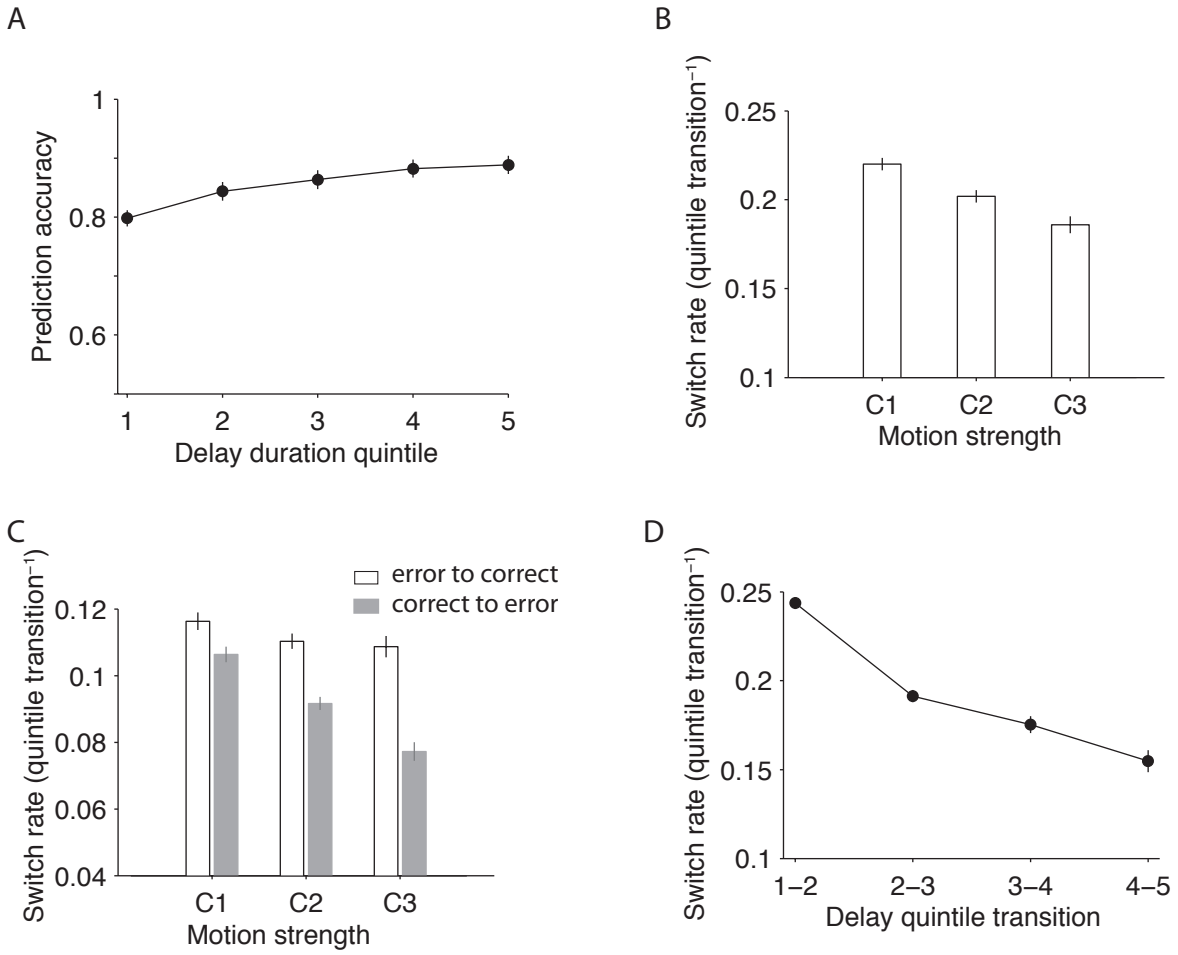

Figure S1. A single discriminant hyperplane is adequate to achieve reliable prediction of choices and changes of mind for all delay quintiles, Related to figure 4. (**A-D**) Same as Fig. 4A-D but for a single logistic model trained and cross-validated for the last 87-100 ms of the delay period of all trials. See Experimental Procedures for details.

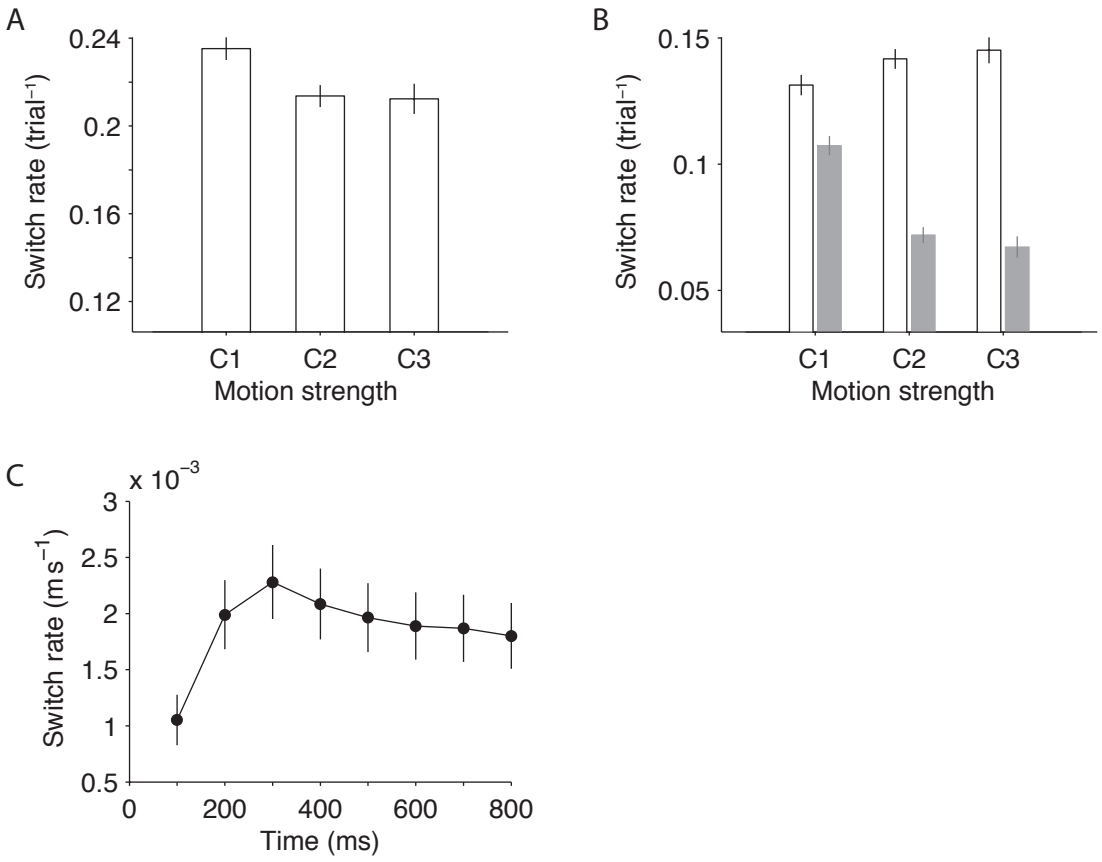

Figure S2. Changes of model DV during motion viewing conform to expected behavioral properties of changes of mind, Related to figure 4. (**A-C**) Same as Fig. 4B-D but for the motion-viewing period. See Experimental Procedures and Results for details.

Supplemental Experimental Procedures

We recorded from populations of neurons in the prearcuate gyrus of two macaque monkeys while they performed a direction discrimination task. All training, surgery, and recording procedures conformed to the National Institutes of Health Guides for the Care and Use of Laboratory Animals and were approved by the Stanford University Animal Care and Use Committee. Due to the similarity of results across the monkeys we pooled the data for all analyses to increase statistical power.

Behavioral task. Figure 1A illustrates the sequence of events on each trial. Each trial began with the appearance of a central fixation point (FP; 0.3° diameter) at the center of the display monitor. The monkey was required to maintain gaze within ±1.5° of FP as long as it was visible on the screen. Eye position was measured with a scleral search coil (CNC Engineering, Seattle, WA), and inappropriate fixation breaks resulted in termination of the trial.

After the monkey fixated on the central fixation point, two targets appeared on the screen (T_1 and T_2). After a 250 ms delay, a random dot motion stimulus was presented for 800 ms and was followed by a delay period of variable duration. At the end of the delay period the FP disappeared (Go cue), instructing the monkey to report the perceived motion direction by making a saccadic eye movement to one of the targets. For a valid response the monkey's saccade was required to land within 2-4° of the target (depending on target eccentricity). In 10 of 15 sessions the two targets were positioned on opposite sides of the screen (T1 contralateral, T2 ipsilateral). On the remaining 5 sessions both targets were positioned contralateral to the recorded hemisphere (T1 and T2 were randomly assigned). On each trial, motion direction was either toward T1 or T2. We controlled the difficulty of the trials by varying the percentage of dots moving coherently in the same direction (motion strength or coherence) as described previously [S1, S2]. The set of motion strengths for each monkey were chosen to afford a wide range of accuracies, from chance to perfection. For monkey 1, the set included 0%, 2.5%, 5%, 10%, 20%, and 40% coherence. For monkey 2, the set included 0%, 1.2%, 2.4%, 4.8%, 9.6%, 19.2%, and 38.4% coherence in most sessions. For two sessions we tested slightly different sets: 0%, 6%, 12%, 24%, and 48% coherence in one session, and 0%, 1%, 2%, 4%, 8%, 16%, and 32% coherence in the other. The motion direction and strength varied randomly from trial to trial, but were fixed within each trial. The monkey received a liquid reward for choosing the target that corresponded to the motion direction. For 0% motion strength the monkey was rewarded randomly on half of the completed trials irrespective of the direction of the choice.

The variability of the delay period duration plays a crucial role in our analyses because it provides an objective means to test the accuracy of our neuronal model predictions about the subject's impending choice. Different delay durations were used in various sessions, permitting useful tests of the robustness of our results. In seven sessions the delay duration of each trial was drawn randomly from these five values: 323 ms, 510 ms, 698 ms, 885 ms, and 1073 ms. In six sessions the delay durations were 673 ms, 760 ms, 848 ms, 935 ms, and 1023 ms. In one session they were 473 ms, 560 ms, 648 ms, 735 ms, and 823 ms; and in the last session they were drawn randomly from several discrete values in the range 300-1500 ms. None of our results strongly depend on the exact delay durations used in each session. We therefore present aggregated results across sessions.

The 15 sessions used in this study were chosen based only on the reliability of recordings, number of trials (>1000), and number of recorded units (>150). The dataset consists of 20938 trials and 3257 units.

Neural recording. The monkeys were implanted with 96-channel microelectrode arrays (electrode length=1.5 mm; spacing=0.4 mm; Blackrock Microsystems, Salt Lake City, UT) in the prearcuate gyrus (Fig. 1B). Neural spike waveforms were saved online (sampling rate, 30 kHz) and sorted offline (Plexon Inc., Dallas, TX). To improve the quality of sorting we used customized algorithms to remove recording artifacts that were registered by a large number of electrodes. Also, we merged redundant spike waveform clusters based on waveform shapes, firing rates and inter-spike intervals. We identified 100-250 single- and multi-units in each session (median=219). Throughout the paper we use the term 'units' to refer to both isolated single neurons and multi-units. All units were retained in our analyses irrespective of their selectivity.

Data analysis. We quantified the time-varying firing rate of each unit on each trial by counting the number of spikes in a sliding 100 ms window (step size=20 ms). We used an L1-regularized logistic regression [S3] to predict the monkey's choice based on neural responses on each trial:

$$Logit\left[P_t(T_1)\right] = \beta_0(t) + \sum_{i=1}^{n} \beta_i(t) r_i(t) \qquad \text{(Equation S1)}$$

where $r_i(t)$ is the firing rate of unit i at time t, n is the number of recorded units and the β coefficients are model parameters. L1-regularization imposes a constraint on the L^1-norm of the coefficients to avoid overfitting. The model was cross-validated by using 90% of trials in each session as 'training set' for fitting the parameters and the remaining 10% as 'test set' to measure the model's prediction accuracy. The best regularization parameter of the model was found by a 10-fold cross-validation within the training set. At any moment in time the model predicts a T_1 choice if $Logit\left[P(T_1)\right] > 0$ and a T_2 choice if $Logit\left[P(T_1)\right] < 0$. The model prediction is correct if it matches the monkey's actual choice at the end of the trial. Fig. 2A shows the model prediction accuracy averaged across sessions. We used a similar logistic regression to gauge the prediction accuracy of individual units:

$$Logit\left[P_{t,i}(T_1)\right] = \beta_0(t) + \beta_1(t) r_i(t) \qquad \text{(Equation S2)}$$

To compare individual units with the population (Fig. 2B-C), we analyzed data from the 100 ms window immediately before the Go cue.

The logistic regression of Equation S1 essentially finds the hyperplane that best separates the population response patterns corresponding to the two choices. The population response pattern at each moment can be envisioned as a point in a high-dimensional space whose axes are the firing rates of individual units. The distance of this point from the discriminant hyperplane (the right-hand side of Equation S1) represents the model belief about the

upcoming choice ($Logit\left[P_t\left(T_1\right)\right]$, the left-hand side of Equation S1). A small distance corresponds to a weak belief and a large distance corresponds to a strong belief. We call this distance the 'model decision variable' (DV) and use the changes in the sign of the DV to identify candidate 'changes of mind' (CoM) for the monkey (Fig. 3C). This approximation is valid especially where the model predicts the monkey's choice accurately.

Our criterion for detecting possible CoM—a simply sign change in the DV—is lenient. It ensures that actual CoM's are not missed, but it can include spurious CoM's due to neural noise or the imperfection of the logistic classifier. We have explored more stringent and complex criteria. For example, a change of mind can be defined as a swing from high certainty for one choice (e.g. large positive DV) to another (e.g. large negative DV). These more stringent criteria have additional degrees of freedom (e.g., criterion on the magnitude of DV) and can be fine tuned to reduce the number of detected CoM's. We explored this space, but the results reported in this paper are not critically dependent on the choice of criteria. For all analyses in this paper, therefore, we employed the simple sign change criterion to avoid additional degrees of freedom and fine-tuning of results.

To determine whether putative neural CoM's conformed to properties expected from prior studies of behavioral changes of mind [S4, S5], we analyzed neural CoM statistics during the delay period (after the dots and before the Go cue) when the model prediction accuracy was above 75% (Figs. 2A and 4A). We first divided the trials of each session into quintiles based on the length of the delay period. As explained above, in 14 of the 15 sessions the delay period was chosen randomly from five distinct values. Therefore the trials in each quintile of a session had identical delays and our grouping did not create spurious boundaries or mix trials with variable delay durations. In contrast to the "sliding window" analysis described above (e.g. Fig. 3), here we calculated the predicted decision (sign of the DV) independently for each delay period quintile. We retrained the logistic model (Equation S1) separately for the trials in each quintile using the last 100 ms of their delay period. For the sessions where the time difference between consecutive quintiles was less than 100 ms, we slightly reduced the size of the window for the calculation of firing rates (87 ms) to ensure no overlap between the quintile models. We then calculated the number of neural CoM's observed on each trial. For trials with the shortest delay periods (first quintile) it was impossible (by definition) to detect a CoM since only a single DV was calculated. For trials of the second quintile, a single opportunity for a CoM occurred, two opportunities for trials of the third quintile, and so forth. Importantly, the high overall prediction accuracy of the model (>75% correct) for trials of the shortest duration (first quintile) creates confidence that the DV calculated within each quintile of longer trials accurately estimates the choice the animal would have made had we stopped those trials earlier. It is thus reasonable to consider neural CoM's detected on long trials to be real changes in the decision state of the animal even though we have no direct behavioral readout of the hidden decision state on these trials. Quantitative analyses in Figure 4 (see equations below) measured CoM statistics for those longer-duration trials (second and higher quintiles).

The results presented in this paper were not critically dependent on training separate models for different delay periods. The discriminant hyperplanes calculated for different delay quintiles were closely related to each other. Consequently, training and cross-validating a single model based on the last 87-100 ms of the delay period of all trials replicated all key results (Fig. S1).

To identify candidate CoM's during the motion-viewing period (Fig. S2) we used the changes in the sign of the decision variable, calculated from the models trained on all trials of a session (Fig. 3). In contrast to the delay period, we could not independently verify the choice-predictive accuracy of CoM's during the motion-viewing period because the motion duration was the same for all trials. A priori, candidate CoM's based on only a DV sign change will be less reliable during the motion-viewing interval due to the lower overall accuracy of the model predictions early in the trial (Fig. 2A). To compensate for this reduced accuracy we used a more stringent criterion. To quantify the frequency and direction of CoM for different motion strengths (Fig. S2A-B), we required the sign of DV to persist for 150 ms before and after a sign change ('persistence window') to qualify as a CoM. To quantify the time course of CoM (Fig. S2C), we reduced this requirement to 75 ms to increase the number of independent estimates of the decision state during motion viewing. The trends in Fig. S2A-B are robust to variations of the persistence window. The trend in Fig. S2C, however, is sensitive to the duration of the persistence window and should be interpreted cautiously; larger windows reduce and even abolish the decline of CoM frequency in the late motion-viewing period. This occurs because long persistence windows impose a sterner criterion for measuring decision states and detecting CoM's, which inevitably delays CoM's to later stages of the motion viewing interval and makes the decision state less likely to change once established. We have observed similar sensitivity to window size in simulations (data not shown).

To test whether the frequency of CoM's during the delay period varied with the stimulus strength we used a linear regression model:

$$\eta = \beta_0 + \beta_1 C + \beta_2 q \qquad \text{(Equation S3)}$$

where η is the number of CoM detected by the model in each trial, C is the motion strength, q is the quintile that the trial delay duration belonged to (2 to 5), and β_i are the regression coefficients. Only trials of the second and higher quintiles contributed to the analysis; as described above, the first quintile could not have a CoM in the delay period. q was included in the regression to control for the increased probability of CoM detection due to increased number of quintile transitions for longer delay periods.

We used a related linear regression to test whether CoM's were more likely to change the monkey's response from an incorrect to a correct choice for stronger stimuli:

$$\Delta s = \beta_0 + \beta_1 C + \beta_2 q \qquad \text{(Equation S4)}$$

where Δs is the difference between the number of CoM's that move the choice prediction from incorrect to correct and vice versa ($\Delta s > 0$ implies more incorrect to correct). This analysis focused on trials with $C > 0$ in which at least one CoM was detected. Trials with $C = 0$ were excluded because of ambiguity in the definition of a correct response. The null hypothesis is that Δs does not change with motion strength ($H_0 : \beta_1 = 0$). After rejecting the null hypothesis via the linear regression analysis, we used a sign rank test to show that the

median of Δs was larger than zero across all trials used in the regression analysis (significant prevalence of incorrect to correct changes).

To test whether the overall probability of being correct was larger on trials in which CoM's were detected we used the following logistic regression:

$$Logit\left[P(cor)\right] = \beta_0 + \beta_1 C + \beta_2 I + \beta_3 q \qquad \text{(Equation S5)}$$

where I is an indicator variable (0 for trials with no CoM and 1 for trials with CoM). C and q are the motion strength and delay duration quintile, respectively (same as in Equation S3). $\beta_2 > 0$ indicates that the subject was correct more frequently on trials in which CoM's were detected.

We tested the dependence of the probability of changes of mind on time using a logistic regression:

$$Logit\left[P(switch)\right] = \beta_0 + \beta_1 C + \beta_2 q' \qquad \text{(Equation S6)}$$

where q' is the delay quintile in which a CoM could be detected minus one. Only trials in the second or higher quintiles contributed to this analysis because at least two delay bins were required to detect a CoM, as described above. Each trial contributed as many data points as permitted by the length of its delay period (maximum=4). The null hypothesis is that the probability of observing a switch does not depend on time ($H_0 : \beta_2 = 0$).

All completed trials (correct and incorrect) were included in the calculation of discriminant hyperplane and subsequent analyses. The grouping of motion strengths to C_1 ($C \leq 6\%$), C_2 ($6\% < C \leq 20\%$), and C_3 ($C > 20\%$) in Fig. 4, S1, and S2 is for illustrative purposes only. All statistical analyses that are mentioned above were performed using the actual motion strengths of the trials.

Supplemental References

S1. Britten, K.H., Shadlen, M.N., Newsome, W.T., and Movshon, J.A. (1992). The analysis of visual motion: a comparison of neuronal and psychophysical performance. J. Neurosci. *12*, 4745-4765.

S2. Kiani, R., Hanks, T.D., and Shadlen, M.N. (2008). Bounded integration in parietal cortex underlies decisions even when viewing duration is dictated by the environment. J. Neurosci. *28*, 3017-3029.

S3. Hastie, T., Tibshirani, R., and Friedman, J. (2008). The elements of statistical learning, 2nd Edition, (New York: Springer).

S4. Resulaj, A., Kiani, R., Wolpert, D.M., and Shadlen, M.N. (2009). Changes of mind in decision-making. Nature *461*, 263-266.

S5. Rabbitt, P.M. (1966). Errors and error correction in choice-response tasks. J Exp Psychol *71*, 264-272.